Evaluation of the Segment Anything Model for post-blast rock fragmentation analysis: A multi-method comparative study at an open-pit gold mine

by I.N. Aslam[1], M.S. Perdana[1], H. Harisman[1], F. Aliva[1], N.A. Putri[1], R. Ayuni[1]

Affiliation:
[1] Mining Engineering Program, Faculty of Engineering, Universitas Syiah Kuala, Banda Aceh, Indonesia

Correspondence to:
I.N. Aslam

Email:
izzanaslam@usk.ac.id

Dates:
Received: 23 Mar. 2026
Revised: 30 Aug. 2025
Accepted: 30 Sep. 2026
Published: Oct. 2026

How to cite:
Aslam I.N., Perdana M.S., Harisman H. Aliva F., Putri N.A., Ayuni R. 2026. Evaluation of the Segment Anything Model for post-blast rock fragmentation analysis: A multi-method comparative study at an open-pit gold mine. *Journal of the Southern African Institute of Mining and Metallurgy*, vol. 126, no. 10, pp. 615 – 624

DOI ID:
https://doi.org/10.17159/2411-9717/3941/2026

ORCiD:
I.N. Aslam
https://orcid.org/0000-0002-4163-6115
M.S. Perdana
https://orcid.org/0009-0003-3818-1978
H. Harisman
https://orcid.org/0009-0005-3240-5090
F. Aliva
https://orcid.org/0009-0009-0853-4879
N.A. Putri
https://orcid.org/0009-0003-5896-3926
R. Ayuni
https://orcid.org/0009-0009-8646-9048

Abstract

Accurate assessment of post-blast rock fragmentation is critical for optimising the mining value chain. Conventional methods such as sieve analysis are time-consuming, while commercial image-analysis software requires costly licences and manual intervention. This study presents a multi-method evaluation of Meta's Segment Anything Model for automated segmentation and particle size distribution analysis of post-blast rock fragments at an open-pit gold mine in Sumatra, Indonesia. Four complementary investigations were conducted: a laboratory-scale comparison against Split Desktop, a field-scale comparison against Strayos with excavator digging time correlation, a pixel-level evaluation against WipFrag using drone-captured imagery, and a statistical analysis of fragmentation metrics versus grizzly feeder clean-up time. The Segment Anything Model 2.1 achieved a mean intersection-over-union of 0.75 and Dice coefficient of 0.85 on high-quality patches, with particle size distribution errors reduced by 89% to 99% relative to WipFrag (up to 90 times lower). Linear regression revealed a significant correlation between maximum fragment diameter and grizzly feeder clean-up time (R^2 = 0.618). Analysis across 24 drone images identified over 23 000 fragments, confirming that more than 99% of blasted material passed the 750 mm feeder aperture. Processing time was reduced from 30 minutes to 2 – 5 minutes per image. These findings support the potential of the Segment Anything Model as an open-source tool for rock fragmentation analysis, contributing to operational assessment within the mine-to-mill optimisation framework.

Keywords

rock fragmentation, deep learning segmentation, particle size distribution, mine-to-mill, grizzly feeder, open-pit mining

Introduction

Post-blast rock fragmentation is a critical determinant of overall mining efficiency, directly influencing excavation productivity, haulage costs, and downstream mineral processing performance (Kinyua et al., 2022). The heterogeneous size distribution of blasted fragments, particularly the presence of oversized boulders, creates bottlenecks at multiple stages of the operational chain: boulders increase excavator digging time and energy consumption, cause blockages at grizzly feeders, and necessitate costly secondary breaking operations (Santos et al., 2020; Nikkhah et al., 2022). Seccatore (2019) emphasised that blasting constitutes the initial stage of comminution, underscoring the need for an integrated mine-to-mill approach that optimises fragmentation from the point of detonation through to final processing (Nageshwaraniyer, 2018).

Quantitative assessment of fragmentation quality relies on particle size distribution (PSD) analysis, traditionally performed through sieve analysis. While considered the gold standard for accuracy, sieve analysis is impractical for routine field application due to processing times of 4 – 6 hours per sample and susceptibility to human error. Image-based analysis has emerged as a practical alternative, with commercial software platforms such as WipFrag, Split Desktop, and Strayos offering automated or semi-automated PSD estimation from photographs of muck piles. However, these tools carry significant limitations: WipFrag and Split Desktop exhibit error rates of 32% – 60% on D_{50} values compared to sieve analysis (Maerz et al., 2018; Girdner et al., 2018), require expensive licences, and demand substantial manual delineation effort that introduces operator subjectivity.

Recent advances in deep learning, particularly the development of foundation models for computer vision, offer potential for rock fragmentation analysis as part of the broader adoption of data intelligence in mining. Meta's Segment Anything Model (SAM), introduced by Kirillov et al. (2023), demonstrated strong zero-shot segmentation capabilities across diverse visual domains without task-specific training. Subsequent iterations, SAM 2.0 (Ravi et al., 2025) and SAM 2.1, have achieved significant improvements

in processing speed (6 × faster than SAM 1.0), segmentation accuracy, and robustness to complex visual conditions through enhanced streaming memory mechanisms and improved positional encoding.

Zhao et al. (2024) pioneered the application of SAM for post-blast rock fragmentation identification, demonstrating its zero-shot segmentation capability using 83 images captured at 1 m above ground level. While promising, their study was limited by close-range sampling that provided insufficient spatial coverage for representative PSD assessment. Shan et al. (2024) further validated SAM's potential for drilling rock image segmentation, confirming its analytical depth regarding fragment physical characteristics including size, shape, and distribution.

Despite these encouraging results, several critical research gaps remain. To the authors' knowledge, few studies have systematically compared SAM-based methods against multiple commercial software platforms within a unified analytical framework. The relationship between SAM-derived fragmentation metrics and operational performance indicators such as digging time and grizzly feeder clean-up time has received limited attention. The influence of image quality on SAM segmentation accuracy remains underexplored, and the direct quantitative link between SAM-derived fragment size and clean-up time at the grizzly feeder has not been widely reported.

This paper addresses these gaps through four complementary investigations conducted at an open-pit gold mine in Sumatra, Indonesia. Study 1 provides a controlled laboratory-scale comparison of SAM Rock Fragmentation against Split Desktop. Study 2 evaluates field-scale SAM against Strayos, the mine's commercial fragmentation analysis platform, with correlation analysis to excavator digging time. Study 3 presents a rigorous assessment of SAM 2.1 against WipFrag using drone-captured imagery with pixel-level ground truth. Study 4 investigates the direct relationship between SAM-derived fragmentation metrics and clean-up time at the grizzly feeder. The studies employed different SAM implementations reflecting the chronological development of the research program: Study 1 used SAM Rock Fragmentation, an open-source tool built on SAM 1.0, as this was the version available when the laboratory-scale investigation commenced. Studies 2, 3, and 4 used SAM 2.1 (the sam2_hiera_large checkpoint), which became available during the field-scale phase and offered improved segmentation accuracy and processing speed. Together, these investigations provide a multi-method evaluation of SAM's viability as an open-source tool for fragmentation analysis within the mine-to-mill optimization framework.



Figure 1—Aerial drone image of a post-blast area captured at 28 m altitude

Methodology

Study area

All investigations were conducted at an open-pit gold mine in Sumatra, Indonesia. The mine is situated along the Sumatra Fault Zone, a major geological structure associated with oblique subduction of the Indo-Australian plate. The deposit is classified as a high-sulfidation epithermal gold-silver system, with principal rock types including basalt andesite, volcanic breccia, porphyritic andesite, and phreatomagmatic diatreme breccia. The open-pit extraction employs conventional drill-and-blast methods with hydraulic excavators for loading. Detailed blast-design parameters (bench height, burden, spacing, hole diameter, explosive type, powder factor, and initiation practice) were not available for publication due to confidentiality requirements of the mine operator. The absence of these parameters precludes direct evaluation of blast-design effectiveness and constitutes a limitation of this study. A representative aerial view of a post-blast area at the study mine, captured at 28 m altitude, is presented in Figure 1.

The mine utilises a grizzly feeder system with an aperture of 750 mm (mine operational specification, personal communication) to screen incoming material before primary crushing. Fragments exceeding this aperture are classified as boulders requiring secondary breaking, making the 750 mm threshold a critical operational benchmark for evaluating blast effectiveness.

Study 1: SAM Rock Fragmentation versus Split Desktop (laboratory scale)

Ten photographs of rock pile fragmentation models were captured at standardised 500 × 500 pixel resolution from rock piles with known fragment sizes. Each image was analysed using three methods: manual measurement of individual fragment diameters using a digital calliper as ground truth (each visible fragment in the photograph was measured and recorded individually), Split Desktop with and without manual delineation, and SAM Rock Fragmentation, an open-source implementation based on SAM 1.0 (Morocho, 2023). For each method, P20, P50, and P80 values were computed and compared against ground truth using root mean square error (RMSE). Split Desktop analyses required approximately 30 minutes per image, including manual corrections, while SAM Rock Fragmentation operated fully automatically in approximately 5 minutes per image. The sample size of ten photographs was selected for an exploratory comparative study designed to evaluate method agreement rather than to characterise a population. As the primary objective was to compare the relative accuracy of three PSD estimation methods against the same ground truth, the ten images served as paired measurement cases rather than independent statistical samples.

Fragment sizes were derived from the 2D segmented masks by computing the equivalent circular diameter for each fragment, defined as d = (4A/π)^0.5, where A is the pixel area of the segmented mask. This equivalent diameter represents the diameter of a circle with the same area as the irregular 2D projection of the fragment. The resulting size distributions are number-weighted (each fragment counted equally regardless of mass or volume) and represent projected 2D dimensions rather than true 3D particle sizes, which is a recognised limitation of all image-based fragmentation analysis methods. Pixel-based diameters were converted to real-world dimensions using the computed GSD. The Rosin-Rammler distribution model was then applied to characterise the cumulative PSD curves, expressed as $Y = 1 - \exp[-(x/xe)^n]$,

where Y is the cumulative fraction passing, xe is the characteristic particle size, and n is the uniformity index.

Study 2: SAM versus Strayos with digging time correlation (field scale)

Drone imagery was captured at 28 m altitude above post-blast areas at the study mine using a DJI Mavic drone equipped with a camera having a focal length of 2.86 cm and sensor width of 0.132 cm. Each full-resolution image was cropped into nine sub-images for computational tractability. Ground sampling distance (GSD) was calculated for each sub-image using GSD = (flight height / focal length) × pixel size, yielding values ranging from 0.089 to 0.154 cm/pixel. The GSD calculation assumes a nadir camera orientation and flat terrain; no corrections were applied for terrain relief, camera tilt, or lens distortion. This represents a limitation, as surface undulations in the muck pile can introduce localised scale errors.

SAM segmentation was performed on each sub-image, and the resulting fragment masks were converted from pixel-based measurements to real-world dimensions using the computed GSD. PSD curves were generated following the Rosin-Rammler model and directly compared against PSD outputs from Strayos, the mine's licensed cloud-based fragmentation analysis platform. Additionally, excavator digging time data from the corresponding loading points were collected to establish correlations between fragmentation characteristics and operational performance. The interquartile range (IQR) method was employed to identify and remove outliers from the equivalent circular diameter data. Fragments with diameters falling below Q1 − 1.5 × IQR or above Q3 + 1.5 × IQR were classified as outliers and excluded from the PSD analysis. The exact number of fragments removed per image was not recorded during the original analysis, which is acknowledged as a reporting limitation. The IQR method was selected because it is non-parametric and does not assume normality, making it appropriate for fragment size distributions that typically follow lognormal or Rosin-Rammler distributions rather than Gaussian distributions.

Study 3: SAM 2.1 versus WipFrag with pixel-level ground truth

Twenty-four drone images (5472 × 3648 pixels) were captured at 28 m altitude across multiple post-blast areas. Each image was subdivided into overlapping square tiles (1216 × 1216 pixels, 20% overlap) for computational tractability, yielding approximately 25 tiles per image and 600 analysis patches in total. Prior to segmentation, all tiles were enhanced using contrast limited adaptive histogram equalisation (CLAHE) in the LAB colour space, with the clip limit optimised to maintain a peak signal-to-noise ratio above 30 dB. Four patches were selected for detailed evaluation based on visual quality classification (two high-quality and two low-quality). This purposive selection from 600 available patches introduces a risk of selection bias, as the chosen patches may not be representative of the full dataset. Future work should employ stratified random sampling or cross-validation across a larger subset of patches to provide more robust performance estimates: Patches 2 and 3 (high quality, with distinct texture, strong contrast, and dominant rock features) and Patches 0 and 16 (low quality, with blurred texture, low contrast, and minimal distinguishable rock features).

For each selected patch, manual pixel-level segmentation was performed by a single annotator using LabelMe (MIT) to establish ground truth masks. The four patches were purposively selected from the quality extremes of the 600-patch dataset: Patches 2 and 3 representing high-quality conditions and Patches 0 and 16 representing low-quality conditions. The delineation protocol required that only visually distinguishable fragments were labelled, overlapping fragments were delineated as separate objects without merging, and fines that could not be individually resolved were excluded. As only one annotator was involved, inter-rater agreement could not be assessed, and intra-rater repeatability was not tested. Ground truth uncertainty may therefore be present, particularly for fragments with ambiguous boundaries, and this should be considered when interpreting the reported accuracy metrics. SAM 2.1 was applied in fully automatic mode using the SAM2AutomaticMaskGenerator (checkpoint: sam2.1_hiera_large.pt; points_per_side = 128, points_per_batch = 256, pred_iou_thresh = 0.9, stability_score_thresh = 0.95, crop_n_layers = 2, box_nms_thresh = 0.4, min_mask_region_area = 10.0, use_m2m = true). The model was executed on Google Colab with an NVIDIA A100 GPU. WipFrag 3.3 was used as the commercial benchmark. The scale was calibrated using the same ground sampling distance (GSD = 5.676 mm/pixel) applied to the SAM 2.1 analysis, ensuring dimensional consistency between the two methods. Edge detection was performed using the edge detection parameters (EDP) function with the best fit mode set to thorough. No additional manual edge correction was applied beyond the automated EDP output. After segmentation, overlapping masks from adjacent tiles were merged using a polygon union algorithm (Shapely library) with an overlap threshold of 0.2 (20% intersection over the smaller polygon area). Mask contours were simplified using the Ramer-Douglas-Peucker algorithm (epsilon = 0.002 × arc length). Additional post-processing included noise removal (fragments smaller than 5 pixels or larger than 50 000 pixels excluded) and circularity filtering (threshold = 0.5). Segmentation performance was quantified using five metrics: intersection over union (IoU), Dice coefficient, precision, recall, and F1-score. PSD prediction accuracy was assessed using mean absolute error (MAE), mean squared error (MSE), and root mean squared error (RMSE), with additional analysis of deviation at D_{10}, D_{50}, and D_{80} percentiles.

Beyond the patch-level evaluation, SAM 2.1 was deployed on all 24 drone images to analyse full-scale fragmentation characteristics across the mine site. The complete dataset of over 23 000 identified fragments was analysed to generate PSD curves, evaluate blast success against the 750 mm grizzly feeder threshold, and derive operational insights for mine planning.

Study 4: SAM 2.1 segmentation at the run-of-mine bin and clean-up time correlation

A dedicated investigation was conducted to evaluate the relationship between SAM-derived fragmentation metrics and clean-up time at the grizzly feeder. The grizzly feeder at the study mine features a screen aperture of 75 cm, with steel bars of 35 cm width that serve as the calibration reference for pixel-to-real-world conversion. Clean-up time is defined as the duration required to clear material that becomes trapped between the grizzly bars, causing bottlenecks in the feeding process. A total of 45 clean-up time records were collected as primary data through direct observation at the run-of-mine bin.

CCTV footage from the run-of-mine bin area was used to capture images of rock fragments on the grizzly feeder surface. From the 45 records, 23 images (51%) met the quality criteria for segmentation analysis. The remaining 22 images were excluded due to excessive motion blur, partial occlusion of the grizzly feeder surface by the excavator bucket, or insufficient lighting conditions

that prevented reliable fragment boundary identification. The exclusion of nearly half the records may introduce selection bias towards clearer imaging conditions, and the results should be interpreted accordingly. SAM 2.1 (checkpoint: sam2_hiera_large.pt; points_per_side = 64, pred_iou_thresh = 0.75, stability_score_thresh = 0.92, crop_n_layers = 1, min_mask_region_area = 15.0; NVIDIA T4 GPU) was deployed to segment rock fragments in each image, with the grizzly feeder steel bar (35 cm) used as the calibration object for converting pixel-based measurements to real-world dimensions. The calibration assumes the steel bar and rock fragments are at the same depth plane relative to the camera. In practice, CCTV perspective distortion, camera angle, and differences in depth between the bar surface and the rock fragments can introduce measurement uncertainty, which was not quantified in this study and represents a limitation of the clean-up time analysis.

Statistical correlation analysis was performed using linear regression to evaluate two relationships: maximum fragment diameter versus clean-up time, and average diameter of fragments exceeding 75 cm versus clean-up time. The coefficient of determination (R^2) was computed to quantify the explanatory power of each regression model.

Results and discussion

Study 1: SAM Rock Fragmentation versus Split Desktop

Table 1 presents the RMSE values for each of the ten fragmentation model photographs across three analytical methods. Split Desktop with manual delineation exhibited the highest variability and largest errors, with RMSE values ranging from 2.03 to 17.26, reflecting the inherent subjectivity of manual edge delineation. Several photographs (Photos 2, 3, 6, and 9) yielded RMSE values exceeding 10, indicating substantial inaccuracy.

Split Desktop without manual delineation demonstrated markedly improved performance, with RMSE values ranging from 0.96 to 5.96, attributable to the consistency of its automated algorithmic approach. SAM Rock Fragmentation achieved RMSE values between 2.80 and 4.82, showing a narrower error range than either Split Desktop configuration. The overall PSD curves generated by SAM rRock fFragmentation more closely approximated the manual ground truth curves, particularly for fragments in the 0 mm – 100 mm range.

A notable exception occurred with Photo 10, where Split Desktop with delineation outperformed both automated methods. This anomaly was attributed to a higher zoom level during image capture, suggesting that standardised imaging protocols are essential for consistent automated analysis. Overall, both SAM Rock Fragmentation and Split Desktop without delineation produced reliable results, with SAM offering the advantage of fully automated processing at approximately one-sixth of the processing time. A representative comparison of the particle size distribution curves from the three methods against manual ground truth is shown in Figure 2, illustrating the closer agreement of the SAM Rock Fragmentation curve with the actual measurements.

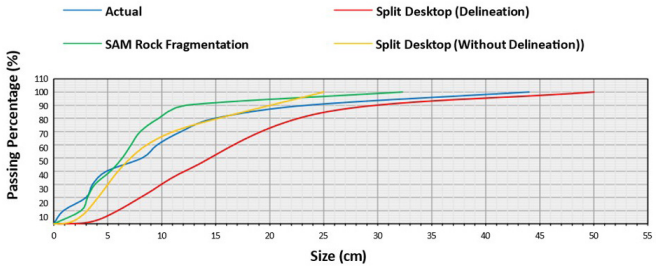

Figure 2—Comparison of particle size distribution curves from manual measurement (blue), Split Desktop with delineation (red), Split Desktop without delineation (orange), and SAM Rock Fragmentation (green) for a representative sample

Table 1

RMSE comparison of Split Desktop and SAM Rock Fragmentation against manual ground truth

Photo	Split Desktop	Split Desktop	SAM Rock Fragmentation
1	6.39	0.96	3.18
2	17.26	1.18	3.51
3	13.16	1.76	3.86
4	8.14	4.49	4.37
5	8.12	2.69	3.36
6	11.99	2.28	4.02
7	8.51	2.64	2.80
8	6.62	2.53	2.97
9	11.64	4.81	4.72
10	2.03	5.96	4.82

Study 2: SAM versus Strayos and digging time correlation

The field-scale deployment of SAM on drone imagery from the study mine demonstrated the model's capability to process large-scale post-blast areas. After segmentation and outlier removal using the interquartile range method, the PSD analysis yielded

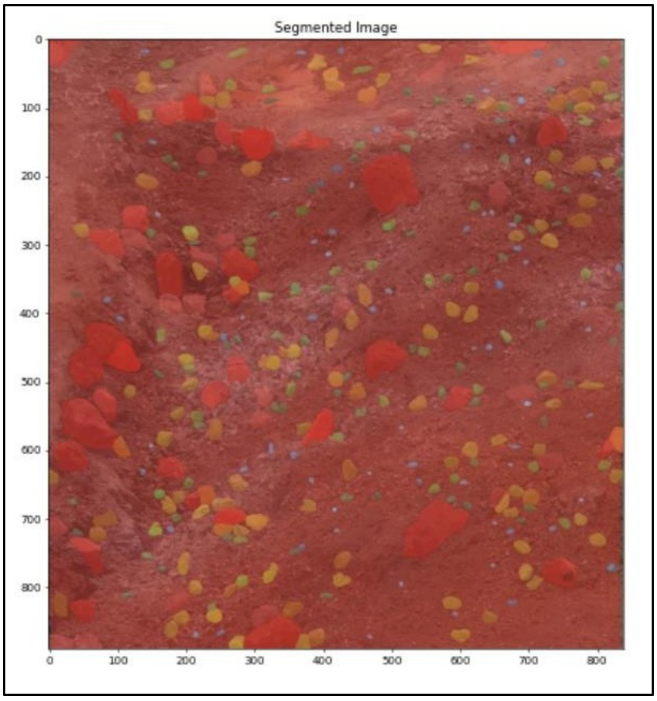

Figure 3—SAM segmentation output showing individual rock fragments identified by colour-coded masks

representative fragment size distributions. For a representative area (Image 1), the analysis identified P_{10} = 1.46 cm, P_{50} = 3.55 cm, and P_{80} = 5.28 cm, indicating a fragmentation profile dominated by fine to medium fragments well-suited for the mine's processing requirements. The SAM segmentation output for this area is presented in Figure 3, where individual rock fragments are distinguished by colour-coded masks.

Comparison with Strayos outputs was limited to a qualitative assessment of PSD trends because the Strayos platform operates as a cloud-based service that does not permit export of raw fragment-level data for independent statistical analysis. Within this constraint, both methods identified broadly similar proportions of material in the fine, medium, and coarse fractions. However, SAM exhibited a tendency to segment fine particles more comprehensively than Strayos, particularly in areas with complex textures. The SAM model occasionally produced outliers at the P_{100} percentile, where very large apparent fragment sizes resulted from the model's inability to distinguish fine, closely packed fragments from a single large surface.

Table 2

Average segment error metrics of SAM 2.1 by image quality category

Patch quality	IoU	Dice	Precision	Recall	F1-score
High	0.7452	0.8535	0.7937	0.9247	0.8535
Low	0.4827	0.5649	0.3845	0.5521	0.4304
Δ (%)	−35.2	−33.8	−51.6	−40.3	−49.6

Analysis of the relationship between SAM-derived fragmentation metrics and excavator digging time indicated that areas with smaller P_{50} and P_{80} values generally exhibited shorter digging times, consistent with the established understanding that finer fragmentation reduces excavation resistance and improves

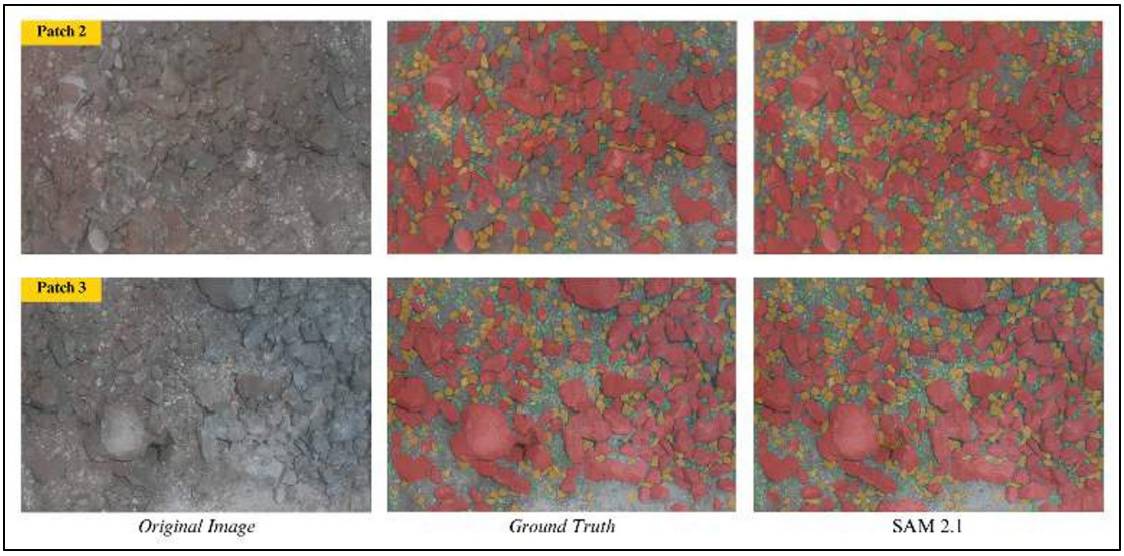

Figure 4—Segmentation results on high-quality patches: original image (left), manual ground truth (centre), and SAM 2.1 output (right) for Patch 2 (top) and Patch 3 (bottom)

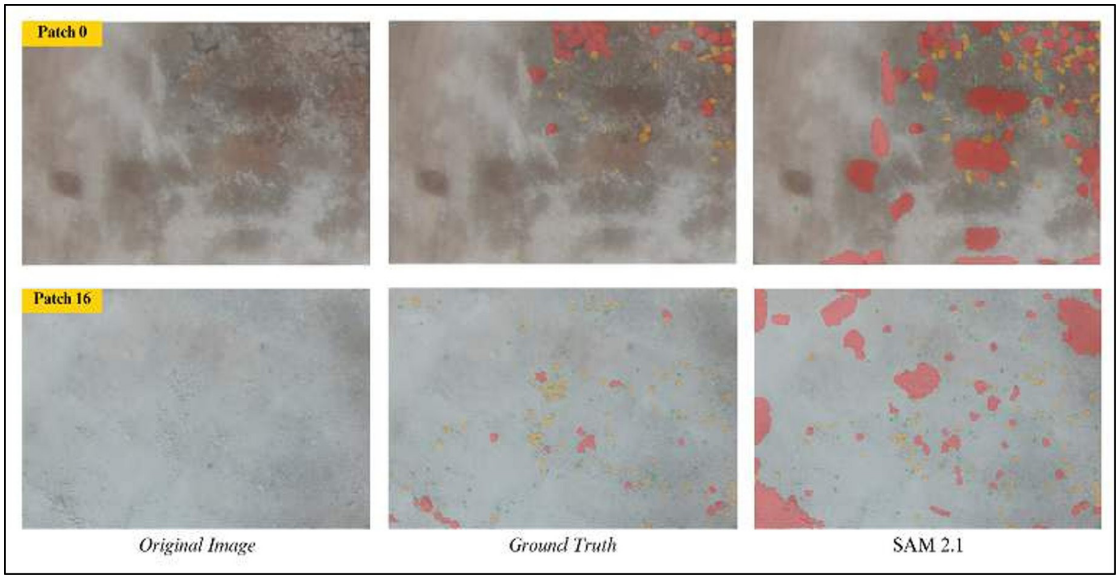

Figure 5—Segmentation results on low-quality patches: original image (left), manual ground truth (centre), and SAM 2.1 output (right) for Patch 0 (top) and Patch 16 (bottom)

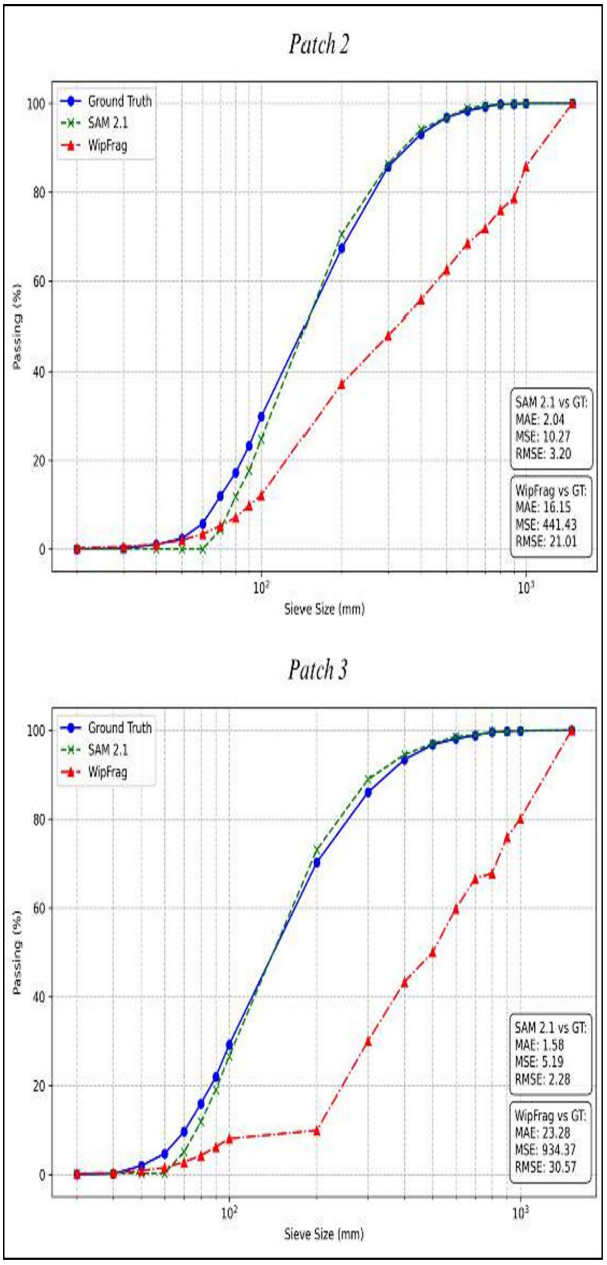

Figure 6—Particle size distribution curves of SAM 2.1 (green), WipFrag (red), and ground truth (blue) on high-quality patches

Table 3
Comparative PSD error metrics: SAM 2.1 versus WipFrag

Method	Quality	MAE	MSE	RMSE
SAM 2.1	High	1.78	7.60	2.71
SAM 2.1	Low	4.65	39.58	6.15
WipFrag	High	19.72	687.90	25.79
WipFrag	Low	18.49	546.44	23.37

bucket fill factors (Kinyua et al., 2022). However, this observation was not supported by formal regression analysis (regression coefficients, p-values, and confidence intervals were not computed), and should therefore be interpreted as a preliminary qualitative indication rather than a statistically validated relationship.
The absence of quantitative digging-time correlation statistics constitutes a limitation of Study 2. Future work should collect paired digging-time and PSD data with sufficient sample size to enable formal regression analysis and hypothesis testing.

Study 3: SAM 2.1 segmentation accuracy versus WipFrag

Segment error metrics

Table 2 summarises the pixel-level segmentation performance of SAM 2.1 across high- and low-quality patches. On high-quality patches, SAM 2.1 achieved an average IoU of 0.7452 and Dice coefficient of 0.8535, indicating that approximately 74.5% of segmented areas aligned with ground truth, with over 85% overlap in detected regions. Recall values averaging 0.9247 confirmed that the model captured nearly all relevant rock fragments, while precision of 0.7937 indicated limited false-positive classification of background as rock. The visual comparison between the original images, manual ground truth, and SAM 2.1 segmentation output on the high-quality patches, is presented in Figure 4, confirming the close correspondence reflected in the quantitative metrics.

Performance on low-quality patches declined substantially, with average IoU dropping to 0.4827 (a 35.2% reduction) and precision falling to 0.3845 (a 51.6% reduction). This degradation reflects the fundamental challenge of segmenting rock fragments in images with blurred textures, low contrast, and minimal visual differentiation between fragments and background. Over-

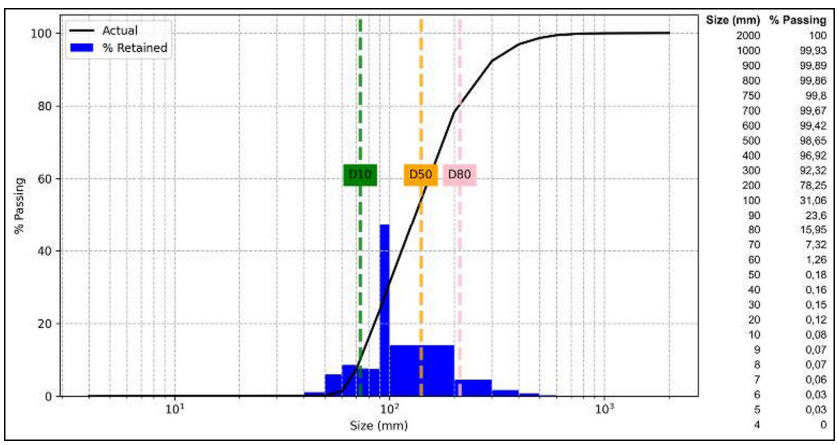

Figure 7—Full-scale particle size distribution curve from SAM 2.1 analysis showing cumulative percentage passing versus screen size for a complete post-blast drone image (14 628 fragments identified)

Table 4
Summary of blast evaluation results from SAM 2.1 analysis (selected images)

Image	D_{10} (mm)	D_{50} (mm)	D_{80} (mm)	Passing ≤ 750 mm (%)	Boulders > 750 mm
1	73.10	140.13	212.41	99.80	29
2	53.48	106.33	186.53	99.46	48
3	60.57	133.39	213.00	99.47	58
4	48.87	106.40	188.38	99.78	30
5	50.97	115.33	195.11	99.88	16
9	53.19	113.19	190.67	99.91	12
10	62.14	131.59	213.82	99.11	86
13	62.17	138.43	230.88	99.55	57

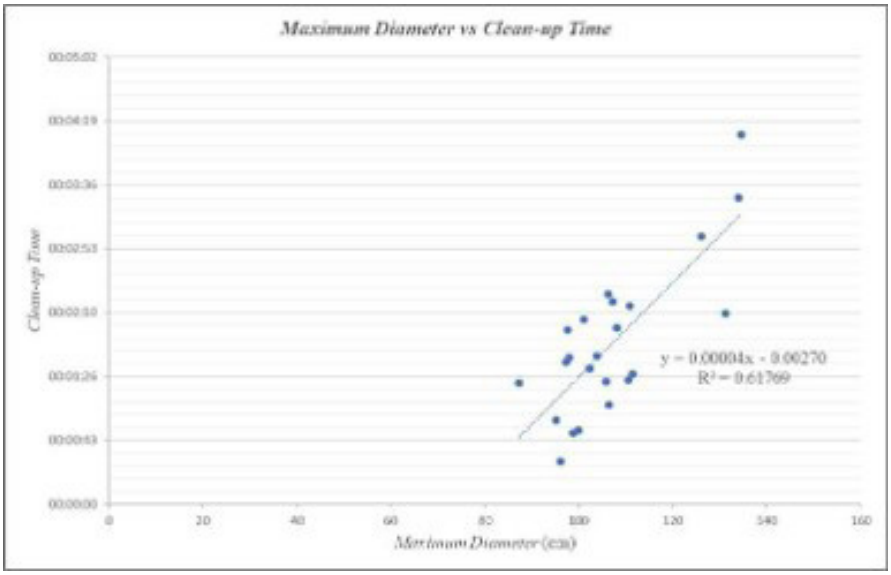

Figure 8—Linear regression of maximum fragment diameter versus grizzly feeder clean-up time (R^2 = 0.618, n = 23)

segmentation of background areas was observed, consistent with SAM 2.1's architecture as a general-purpose segmentation model without domain-specific training. The over-segmentation behaviour on low-quality patches is visually evident in Figure 5, where the SAM 2.1 output exhibits excessive classification of background areas as rock fragments compared to the ground truth.

These findings note that foundation models, despite training on diverse large-scale datasets, face difficulties in specialised domains with ambiguous visual characteristics. The 35% – 52% performance degradation across metrics underscores the need for either fine-tuning SAM on mining-specific datasets or implementing preprocessing pipelines to enhance image quality before segmentation.

Particle size distribution error metrics and comparison with WipFrag

Table 3 presents the PSD prediction error metrics for SAM 2.1 and WipFrag across both quality categories. On high-quality patches, SAM 2.1 achieved remarkably low error values (MAE = 1.78, MSE = 7.60, RMSE = 2.71), substantially outperforming WipFrag (MAE = 19.72, MSE = 687.90, RMSE = 25.79). SAM 2.1 reduced MAE by 91%, MSE by 99%, and RMSE by 90% compared to WipFrag on these patches, corresponding to WipFrag errors being 11.1, 90.5, and 9.5 times larger than those of SAM 2.1, respectively.

Table 5
PSD evaluation at grizzly feeder (selected images)

Image	P_{50} (cm)	P_{80} (cm)	Passing ≤ 75 cm (%)
1	19.91	31.28	97.87
3	24.22	40.00	92.97
7	25.64	51.90	92.54
11	17.94	28.27	97.93
14	17.77	25.35	98.88
17	17.89	26.60	99.44

Even on low-quality patches, where SAM 2.1 performance degraded (MAE = 4.65, MSE = 39.58, RMSE = 6.15), it maintained substantial superiority over WipFrag (MAE = 18.49, MSE = 546.44, RMSE = 23.37), with error reductions of 75%, 93%, and 74% for MAE, MSE, and RMSE, respectively, corresponding to WipFrag errors being 4.0, 13.8, and 3.8 times larger. The superiority of SAM

2.1 over WipFrag is visually apparent in Figure 6, where the SAM 2.1 particle size distribution curve consistently approximates the ground truth more closely than the WipFrag curve across the full range of fragment sizes. Analysis of individual PSD percentiles revealed that SAM 2.1 excels at predicting median fragment sizes (D_{50}), with an average error of only 0.87 mm on high-quality patches. However, prediction accuracy was lower at the distribution extremes: D_{10} error averaged 8.88 mm and D_{80} error averaged 13.54 mm on high-quality patches.

The processing time advantage of SAM 2.1 was equally compelling: an average of 2 minutes per patch compared to 30 minutes for WipFrag, representing a 15-fold efficiency improvement.

Full-scale blast evaluation and operational implications

Deployment of SAM 2.1 across 24 drone images yielded comprehensive fragmentation data for operational assessment. Table 4 presents a representative subset of the blast evaluation results. Across all analysed blast areas, the proportion of material passing the 750 mm grizzly feeder aperture ranged from 99.11% to 99.91%, with boulder counts ranging from 12 to 86 per image. These results indicate highly effective blast designs, with minimal requirement for secondary breaking operations.

Average fragment diameters ranged from 106.33 mm to 140.13 mm (D_{50}), with D_{80} values between 186.53 mm and 216.28 mm. The relatively narrow distribution of D_{50} values across different blast locations suggests consistent blast design application, while variations in D_{10} (48.87 mm – 73.10 mm) reflect localised geological heterogeneity. Total fragment counts per image ranged from approximately 8 900 to 14 600, demonstrating SAM 2.1's capacity to process complex scenes with thousands of individual objects. A representative full-scale particle size distribution curve generated from SAM 2.1 analysis of a complete drone image containing 14 628 identified fragments is presented in Figure 7.

These fragmentation characteristics have direct implications for downstream operational efficiency. With P_{80} values consistently below 220 mm and over 99% of material passing the grizzly feeder, the current blast designs support uninterrupted material flow through the processing plant. The small fraction of boulders identified (typically 0.1% – 0.9% of total fragments) suggests that the analysed blasts produced limited oversize relative to the feeder aperture, while providing quantitative data for continuous improvement of blast designs.

The integration of SAM-based PSD analysis into routine operational workflows enables proactive decision-making aligned with good mining practice principles and the broader paradigm of data intelligence for operational risk management in geometallurgy. By providing rapid, automated fragmentation assessment within minutes of drone image capture, mine planners can adjust excavation strategies, allocate secondary breaking resources, and communicate material characteristics to the processing plant in near real-time—a fundamental requirement of the mine-to-mill optimisation concept.

Clean-up time correlation at grizzly feeder

SAM 2.1 segmentation of 23 CCTV images captured at the run-of-mine bin grizzly feeder achieved an average stability score of 94.26%, demonstrating consistent performance in the challenging visual environment of the feeding station. The model successfully identified fragment boundaries in most images, though limitations were observed in cases involving visually complex structures, including occasional misclassification of the grizzly feeder steel bars as rock fragments and difficulty distinguishing individual fragments in densely packed fine material zones.

Table 5 presents a subset of the PSD evaluation results for the grizzly feeder images. The analysis revealed P_{50} values ranging from 17.77 cm to 25.64 cm and P_{80} values from 25.35 cm to 51.90 cm across the 23 datasets. The cumulative percentage of material passing the 75 cm screen aperture ranged from 92.54% to 99.44%, indicating that the vast majority of blasted material could be processed by the grizzly feeder without intervention. However, the remaining 0.5% – 7.5% of material exceeding the screen aperture constituted the boulders responsible for operational delays requiring clean-up procedures.

Linear regression analysis of maximum fragment diameter versus clean-up time yielded the equation $y = 0.00004x - 0.0027$ (where y is clean-up time in minutes and x is maximum fragment diameter in cm; slope = 0.00004 min/cm, intercept = –0.0027 min), with a coefficient of determination $R^2 = 0.618$. The authors acknowledge that R^2 alone does not establish statistical significance; p-values, confidence intervals, and residual diagnostics for the regression models were not computed in the original analysis. Access to the raw data was limited to the regression outputs reported in the aforementioned. Future work should include these inferential statistics to strengthen the basis of these findings. This indicates that the linear model explains 61.8% of the observed variability in clean-up time, indicating a moderately strong linear association between maximum fragment size and clean-up time at the grizzly feeder. The linear regression plot of maximum fragment diameter versus clean-up time is presented in Figure 8, illustrating the positive correlation and the scatter of the 23 data points around the regression line.

The regression of average diameter of fragments exceeding 75 cm versus clean-up time produced the equation $y = 0.00007x - 0.00531$, with $R^2 = 0.501$. While moderately strong, the lower R^2 compared to the maximum diameter analysis suggests that the single largest fragment is a more reliable predictor of clean-up duration than the average size of oversized material. This finding has practical significance for operational risk management; preventing even a single extremely large boulder from reaching the grizzly feeder may be more effective for reducing clean-up time than achieving a general reduction in average boulder size.

The combined findings from the PSD analysis and clean-up time correlation provide actionable intelligence for blast design optimisation as part of a data-driven risk management approach. Since more than 95% of material consistently passes the 75 cm screen, the current blast designs are broadly effective. However, the significant correlation between maximum fragment diameter and clean-up time demonstrates that targeted improvements in blast design to reduce the top-size of fragments could yield measurable reductions in grizzly feeder downtime and overall processing efficiency.

Conclusions

This study presents the most comprehensive multi-method evaluation to date of the Segment Anything Model for post-blast rock fragmentation analysis in open-pit mining. Through four complementary investigations at an open-pit gold mine in Sumatra, Indonesia, the following principal conclusions are drawn.

SAM-based methods consistently outperform commercial fragmentation analysis software across multiple accuracy metrics and operational scales. *SAM 2.1* reduced PSD errors by 74% – 99% compared to *WipFrag* (with *WipFrag* errors being up to 90 times larger), while *SAM Rock Fragmentation* demonstrated comparable

or superior accuracy to *Split Desktop*, particularly when manual delineation subjectivity is considered.

The influence of image quality on segmentation performance is substantial but predictable. *SAM 2.1* segmentation metrics degraded by 35% – 52% between high- and low-quality image patches, with over-segmentation of background areas being the primary failure mode. This finding establishes clear guidelines for operational deployment; standardised drone flight parameters and consistent imaging conditions are prerequisites for reliable automated analysis.

SAM-derived fragmentation metrics demonstrate operational validity through their correlation with excavator digging time and their alignment with *Strayos* outputs at field scale. The analysis of over 23 000 fragments across 24 drone images confirmed that more than 99% of blasted material met the 750 mm grizzly feeder specification, providing actionable intelligence for mine planning.

The statistical analysis of SAM 2.1-derived fragmentation metrics at the grizzly feeder established a significant correlation between maximum fragment diameter and clean-up time (R^2 = 0.618), with a moderately strong relationship also observed for average boulder diameter above 75 cm (R^2 = 0.501). These findings quantitatively demonstrate that SAM-based fragmentation assessment may help anticipate downstream operational bottlenecks, enabling proactive blast design optimisation to minimise grizzly feeder downtime.

The processing efficiency advantage of SAM (2 to 5 minutes per image versus 30 minutes for commercial software), combined with its open-source availability and zero licensing cost, positions it as a transformative data intelligence tool for routine fragmentation assessment. This efficiency enables the near-real-time feedback loop essential for mine-to-mill optimisation, operational risk management, and the integration of smart data into geometallurgical workflows.

Future research should incorporate detailed blast-design parameters (burden, spacing, powder factor, rock-mass classification) to enable direct evaluation of the relationship between blast design and SAM-derived fragmentation metrics. Additional priorities include domain-specific fine-tuning of SAM using mining fragmentation datasets to improve performance on low-quality images, development of cloud-based processing pipelines to overcome local computational limitations, extension of the analysis to quantify the mathematical relationship between SAM-derived PSD and the full mineral processing chain efficiency, and longitudinal studies tracking the impact of SAM-informed blast design adjustments on overall mine productivity and cost reduction.

Acknowledgements

The authors gratefully acknowledge the support of the mining contractor and the mine operator at the study site for providing access to operational data and field facilities. Special appreciation is extended to the drill and blast engineering team for their technical guidance. The authors also thank Mining Engineering Program, Faculty of Engineering, Universitas Syiah Kuala, for institutional support throughout this research.

Credit author statement

I.N. Aslam: Overall project conceptualisation, project management, supervision, methodology, software, formal analysis, project funder.

M.S. Perdana: Conceptualisation for project *SAM 2.1 and WipFrag*, deep learning analysis, and grizzly case, methodology, software, investigation, formal analysis, writing – original draft.

H. Harisman: Supervision, writing – review and editing, formal analysis.

F. Aliva: Investigation for SplitDesktop, formal analysis, writing – original draft.

N.A. Putri: Investigation for *SAM 2.1*, data curation, writing – original draft.

R. Ayuni: Investigation for *SAM 2.1*, writing – review and editing.

References

Data availability: The SAM 2.1 model and code are publicly available through Meta's GitHub repository (https://github.com/facebookresearch/sam2). The SAM Rock Fragmentation tool is available at https://github.com/Yairama/SAM-Rock-Fragmentation. The drone imagery, CCTV images, segmentation masks, and clean-up time data used in this study are not publicly available due to confidentiality agreements with the mine operator. Requests for data access may be directed to the corresponding author.

Girdner, K.K., Kemeny, J.M., Srikant, A., McGill, R. 2018. The split system for analyzing the size distribution of fragmented rock. *In Measurement of Blast Fragmentation* pp. 101-108. Routledge.

Kinyua, E.M., Jianhua, Z., Kasomo, R.M., Mauti, D., Mwangangi, J. 2022. A review of the influence of blast fragmentation on downstream processing of metal ores. *Minerals Engineering*, vol. 186, pp. 107743.

Kirillov, A., Mintun, E., Ravi, N., Mao, H., Rolland, C., Gustafson, L., Xiao, T., Whitehead, S., Berg, A.C., Lo, W.Y., Dollár, P. 2023. October. Segment anything. *In 2023 IEEE/CVF international conference on computer vision (ICCV)* pp. 3992-4003. IEEE.

Maerz, N.H., Palangio, T.C., Franklin, J.A. 2018. WipFrag image based granulometry system. *Proceedings of the FRAGBLAST*, 5, pp.91-99.

Morocho, Y.C. 2023. Yairama/SAM-Rock-Fragmentation. GitHub Repository. https://github.com/Yairama/SAM-Rock-Fragmentation [accessed 10 October 2024].

Nageshwaraniyer, S.S., Kim, K., Son, Y.J. 2018. A mine-to-mill economic analysis model and spectral imaging-based tracking system for a copper mine. *Journal of the Southern African institute of mining and metallurgy,* vol. 118, no. 1, pp.7–14.

Nikkhah, A., Vakylabad, A.B., Hassanzadeh, A., Niedoba, T., Surowiak, A. 2022. An evaluation on the impact of ore fragmented by blasting on mining performance. *Minerals*, vol. 12, no. 2, pp.258.

Ravi, N., Gabeur, V., Hu, Y.T., Hu, R., Ryali, C., Ma, T., Khedr, H., Rädle, R., Rolland, C., Gustafson, L., Mintun, E. 2025. May. Sam 2: Segment anything in images and videos. In International Conference on Learning Representations vol. 2025, pp. 28085–28128.

Santos, D.R.S., Oliveira, M.R.P., Sampaio Filho, I.S., Paiva, R.S. 2020. Alimentação de rock boulders e não britáveis na britagem primária/rock boulders and non-crushable feed in primary crushing. Braz J Dev, vol. 6, no. 9, pp.73384–73399.

Seccatore, J. 2019. A review of the benefits for comminution circuits offered by rock blasting. *REM-International Engineering Journal*, vol. 72, no. 1, pp.141–146.

Shan, L., Liu, Y., Du, K., Paul, S., Zhang, X., Hei, X. 2024. Drilling rock image segmentation and analysis using segment anything model. Advances in Geo-Energy Research, 12(2), pp.89-101.

Zhao, J., Li, D., Yu, Y. 2024. Identification of rock fragments after blasting by using deep learning-based segment anything model. *Minerals*, vol. 14, no. 7, pp.654. ◆

27-27 MAY 2027
DELOITTE, WATERFALL CITY, MIDRAND

6TH DIGITAL TRANSFORMATION IN MINING CONFERENCE 2027

From Digital Ambition to Operational Impact

CAPABILITY DRIVEN.
TECHNOLOGY ENABLED.
PEOPLE POWERED.
IMPACT FOCUSSED.

SAIMM
THE SOUTHERN AFRICAN INSTITUTE OF MINING AND METALLURGY

INTRODUCTION

Mining is undergoing one of the most interesting periods of transformation in its history.

Growing demand for critical minerals, supply chain instability, evolving workforce expectations, and increasing sustainability ambitions are creating opportunities for innovation, collaboration, and new ways of working.

With continued advances in connectivity, sensing, automation and artificial intelligence, mining companies across the world are reimagining how they discover, plan, operate, maintain, and improve their businesses.

The industry has demonstrated that digital technologies can deliver measurable improvements in safety, productivity, reliability, decision-making, and sustainability. The challenge is scaling and sustaining that value across the enterprise through deeper operating model transformation, and a relentless focus on operational impact.

The 5th Digital Transformation in Mining Conference brings together industry leaders, practitioners, researchers, and innovators to share practical experiences, lessons learned, and proven approaches for transforming digital ambition into operational impact.

Whether you are just beginning your digital transformation journey or already scaling enterprise-wide initiatives, this conference will provide valuable insights, practical examples, and opportunities to engage with those leading the transformation of the mining industry.

The conference will also lend support to a people-centric approach to mining modernisation positing that human expertise and intelligent machines collaboration may enable strengthening safety, capability, and operational performance.



CONTACT

FOR FURTHER INFORMATION CONTACT:
Gugu Charlie, Conferences and Events Coordinator
gugu@saimm.co.za
Tel: +27 11 530 0238